DALTON
FULL PAPER

Hydrothermal synthesis, crystal structure, spectroscopic and magnetic properties of $Mn_4(H_2O)_3(SeO_3)_4$ and $Mn_3(H_2O)(SeO_3)_3$

Aitor Larrañaga,[a] José L. Mesa,*[b] José L. Pizarro,[a] R. Olazcuaga,[c] María I. Arriortua[a] and Teófilo Rojo*[b]

[a] *Departamento de Mineralogía-Petrología, Facultad de Ciencias, Universidad del País Vasco, Apdo. 644, E-48080 Bilbao, Spain*
[b] *Departamento de Química Inorgánica, Facultad de Ciencias, Universidad del País Vasco, Apdo. 644, E-48080 Bilbao, Spain. E-mail: qiproapt@lg.ehu.es*
[c] *Institut de Chimie de la Matière Condensée de Bordeaux, 33608 Pessac, France*

Received 7th March 2002, Accepted 18th July 2002
First published as an Advance Article on the web 20th August 2002

Two new manganese(II) selenites with the formula $Mn_4(H_2O)_3(SeO_3)_4$ (**1**) and $Mn_3(H_2O)(SeO_3)_3$ (**2**) have been synthesized by using mild hydrothermal conditions under autogeneous pressure. The crystal structure of both compounds has been solved from single crystal X-ray data. The structures consist of a three-dimensional framework formed by MnO_6 octahedra and $(SeO_3)^{2-}$ selenite anions with trigonal pyramidal geometry. Compound **1** shows the existence of sheets constructed from zig-zag chains linked to MnO_6 octahedra. Compound **2** exhibits zig-zag chains formed by edge-sharing dimeric octahedra which are interconnected by Mn_2O_{10} octahedra. The IR and Raman spectra show the characteristic bands of the selenite anion. Studies of luminescence at 6.0 K and diffuse reflectance spectroscopy have been carried out for both compounds. The *Dq* and Racah parameters are $Dq = 715$, $B = 705$ and $C = 3420$ cm^{-1} for **1** and $Dq = 710$, $B = 700$ and $C = 3425$ cm^{-1} for **2**. The ESR spectra are isotropic with a *g*-value of 2.00(1), which remains unchanged with variation in temperature. Magnetic measurements indicate the presence of antiferromagnetic interactions in both phases.

Introduction

An important area in materials science is the design of compounds with a condensed framework, which can give rise to original physical properties, due to the great number of different cation arrangements that they can exhibit.[1] In this way, the crystal chemistry of selenium(IV) oxo compounds shows abundant structural versatility expressed by the significant number of different compounds. The electronic configuration of the selenium(IV) oxoanion promotes the formation of three bonding electron pairs with the oxygen atoms. Layered or chain structures are common in compounds containing a hydrogenselenite group, whereas three-dimensional structures are basically formed with the $(SeO_3)^{2-}$ selenite anion.[2]

The transition metal–selenium–oxygen system has been the subject of several previous investigations. Several phases have been reported in which the selenium is found in an oxidation state IV. In this way, transition metal compounds with the $(HSeO_3)^-$, $(SeO_3)^{2-}$ and $(Se_2O_5)^{2-}$ oxoanions are known.[3–5] Although a great number of crystal structures related to the selenite compounds have been resolved, studies on the physical properties of the synthesized phases are scarce. The thermal behaviour and IR spectroscopy of several phases have been reported.[6] The $Mn(Se_2O_5)$ compound with a chain structure shows the existence of antiferromagnetic interactions.[6c] At this point, hydrothermal synthetic techniques can provide us with a method to obtain novel and interesting monophonic compounds which only exist over narrow stabilisation ranges.[7] Mild hydrothermal techniques under autogeneous pressure have allowed the attainment of an astonishing variety of inorganic networks templated by organic species;[8] the preparation of two organically templated zinc and iron(III) open framework selenites has been reported.[9]

The aim of our work is focused on the preparation of selenite phases in the Mn(II)–SeO_2–H_2O system by using mild hydrothermal conditions. In this paper we present the crystal structure and spectroscopic and magnetic properties of two new manganese(II) selenites, $Mn_4(H_2O)_3(SeO_3)_4$ and $Mn_3(H_2O)(SeO_3)_3$.

Results and discussion

Crystal structure of compound 1

The crystal structure of **1** consists of a three-dimensional framework formed by MnO_6 octahedra and $(SeO_3)^{2-}$selenite anions with a trigonal pyramidal geometry (Fig. 1a).

Layers interconnected through the selenite anions can be distinguished in the (10−1) plane (Fig. 1a). These sheets are formed by zig-zag intercrossed chains of octahedra along the *b*-axis (Fig. 1b). There are two crystallographically independent chains. These chains are constructed from $Mn(1)Mn(2)O_{10}$ dimeric octahedra which share the O(5)–O(6) and O(1)–O(2) edges, and from $Mn(3)Mn(4)O_{10}$ edge-sharing octahedra with the O(9)–O(11) and O(8)–O(10) common edges. The chains are linked along the [101] direction through the O(3), O(4) and O(7)-oxygen atoms belonging to the $Se(4)O_3$ selenite anions, and through the O(2) and O(8) atoms from the $Se(2)O_3$ group.

Selected bond distances and angles are listed in Tables 1 and 2. The metal–oxygen bond distances in the MnO_6 octahedra have a mean value of 2.20(7) Å. The water molecules are coordinated to the manganese(II) ions through the O(13), O(14) and O(15) atoms, the mean bond length being 2.15(3) Å. This mean distance is slightly smaller than that observed for other oxygen atoms belonging to the selenite anions. The *cis*-O–Mn–O angles range from 68.4(5) to 108.4(2)° and the *trans*-O–Mn–O angles from 150.1(5) to 178.5(6)°. The distortion of the MnO_6 coordination polyhedra from ideal octahedral geometry[10] is less than 13%. The mean value of the selenium–oxygen

DOI: 10.1039/b206515k

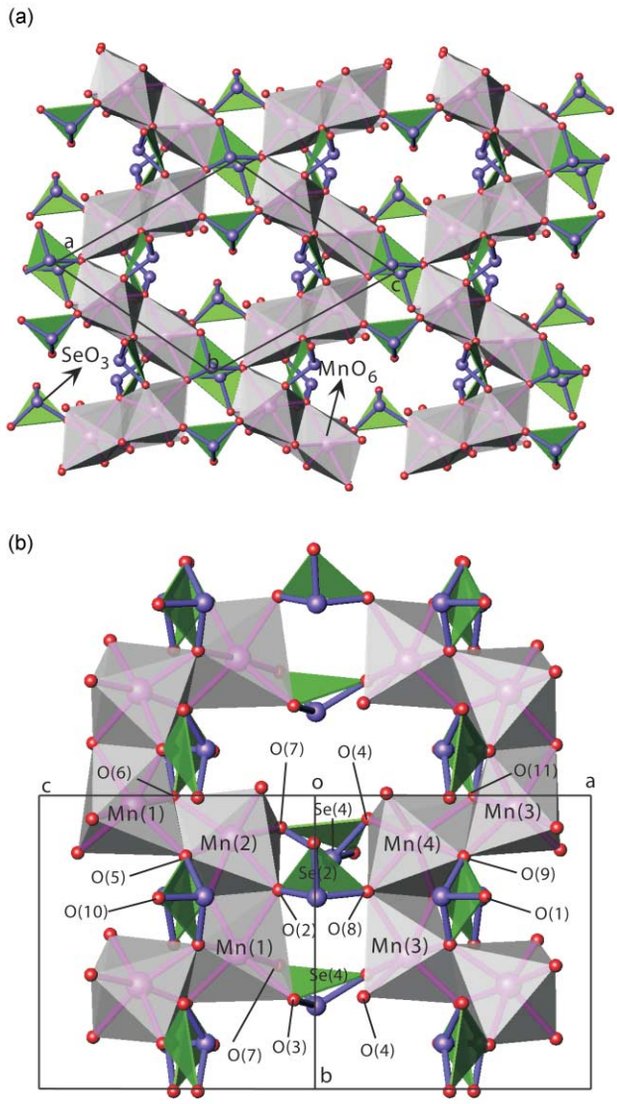

Fig. 1 (a) Polyhedral view of the three-dimensional crystal structure of **1**. (b) Zig-zag chains running along the *b*-axis.

bond lengths is 1.71(3) Å. The O–Se–O bond angles are in the range 92.9(7)–103.8(6)°. The bond valence study[11] for the Se^{4+} and Mn^{2+} cations gives mean values of 3.9 and 1.9 v.u., respectively, in acceptable agreement with the oxidation states of these elements in compound **1**.

Crystal structure of compound 2

Compound **2** crystallizes as a three-dimensional framework formed by MnO_6 octahedra and $(SeO_3)^{2-}$ anions with trigonal pyramidal geometry (Fig. 2a).

The structure along the *a*-axis shows the existence of zig-zag chains formed by edge-sharing dimeric $Mn(4)_2O_{10}$ octahedra linked by common edges to the $Mn(2)O_6$ octahedra (Fig. 2b). These chains are linked along the *c*-axis by edge-sharing $Mn(1)_2O_{10}$ dimeric units, being the connection established through the O(4) and O(2) oxygen atoms of the $Se(2)O_3$ selenite anions. The $Mn(1)O_6$, $Mn(2)O_6$ and $Mn(4)O_6$ octahedra form layers parallel to the (010) plane. These sheets are interconnected by the $Mn(3)O_6$ octahedra, through the O(3) and O(5) atoms belonging to the $Se(1)O_3$ and $Se(2)O_3$ selenites, respectively, and through the O(7), O(8) and O(9) from the $Se(3)O_3$ groups (Fig. 2b).

A list of selected bond lengths and angles is presented in Tables 3 and 4. The mean value of the metal–oxygen bond distances in the MnO_6 octahedra is 2.19(9) Å. The water molecule coordinated to the manganese(II) ion exhibits a bond length of 2.212(4) Å. The *cis*- and *trans*-O–Mn–O angles range from 65.9(1) to 114.7(1)° and from 141.8(1) to 180.0(0)°, respectively. The distortion of the MnO_6 polyhedra from the ideal octahedral symmetry[10] is less than 17%. The mean value of the selenium–oxygen distances is 1.69(2) Å. The O–Se–O bond angles are in the range 94.2(2)–104.8(2)°. The bond valence analysis[11] for the Se^{4+} and Mn^{2+} ions gives mean values of 3.8 and 2.0 v.u., respectively.

Table 1 Selected bond distances (Å) for **1** (e.s.d.s in parentheses)

$Mn(1)O_6$ octahedron		$Mn(2)O_6$ octahedron	
Mn(1)–O(1)	2.13(2)	Mn(2)–O(1)	2.12(2)
Mn(1)–O(2)	2.28(2)	Mn(2)–O(2)	2.20(1)
Mn(1)–O(3)	2.17(1)	Mn(2)–O(5)^{i}	2.25(1)
Mn(1)–O(4)	2.29(1)	Mn(2)–O(7)^{ii}	2.23(2)
Mn(1)–O(5)	2.13(2)	Mn(2)–O(6)^{iii}	2.13(2)
Mn(1)–O(6)^{i}	2.25(1)	Mn(2)–O(13)	2.14(2)
$Mn(3)O_6$ octahedron		$Mn(4)O_6$ octahedron	
Mn(3)–O(7)	2.21(2)	Mn(4)–O(4)^{ii}	2.17(2)
Mn(3)–O(8)	2.29(2)	Mn(4)–O(8)	2.20(2)
Mn(3)–O(9)^{iv}	2.08(2)	Mn(4)–O(9)^{v}	2.24(1)
Mn(3)–O(10)	2.18(2)	Mn(4)–O(10)	2.18(2)
Mn(3)–O(11)^{v}	2.30(1)	Mn(4)–O(11)^{ii}	2.14(1)
Mn(3)–O(14)	2.17(1)	Mn(4)–O(15)	2.15(2)
$Se(1)O_3$ trigonal pyramid		$Se(2)O_3$ trigonal pyramid	
Se(1)–O(1)	1.71(1)	Se(2)–O(2)	1.73(1)
Se(1)–O(9)	1.75(2)	Se(2)–O(8)	1.67(1)
Se(1)–O(11)	1.66(1)	Se(2)–O(12)	1.75(1)
$Se(3)O_3$ trigonal pyramid		$Se(4)O_3$ trigonal pyramid	
Se(3)–O(5)	1.72(1)	Se(4)–O(3)	1.74(1)
Se(3)–O(6)	1.66(2)	Se(4)–O(4)	1.72(2)
Se(3)–O(10)^{iv}	1.70(1)	Se(4)–O(7)	1.75(2)
Metal–metal			
Mn(1)–Mn(2)^{vi}	3.422(6)	Mn(2)–Mn(3)^{ii}	3.565(4)
Mn(1)–Mn(4)^{iv}	3.620(4)	Mn(3)–Mn(4)	3.422(5)

Symmetry codes: i = $-x + 1$, $y - 1/2$, $-z + 2$; ii = $-x$, $y - 1/2$, $-z + 2$; iii = x, $y - 1$, z; iv = $-x$, $y + 1/2$, $-z + 2$; v = x, y, $z + 1$; vi = $-x + 1$, $y + 1/2$, $-z + 2$.

A common structural feature of both three-dimensional compounds **1** and **2** is the presence of cavities delimited by the MnO_6 octahedra and the SeO_3 trigonal pyramidal groups. The lone-pair of the selenite anions points out from the centre of the cavities (see Figs. 1 and 2). The water molecules are directed towards the interior of the cavities in **1** but not in **2**. Notwithstanding, attempts to remove the water molecules under vacuum were unsuccessful. The minimum Se–O distance in the apical direction of the SeO_3 pyramids is 3.49(1) and 3.52(1) Å in compounds **1** and **2**, respectively. These values are in the range found for other selenite compounds.[2]

Infrared, Raman, luminescence and UV-Vis spectroscopies

The infrared and Raman spectra for **1** and **2** show bands corresponding to the stretching and deformation vibrational modes of the water molecules and the $(SeO_3)^{2-}$ anions. The bands obtained from both the IR and Raman spectra are given in Table 5. The positions observed for these vibrational modes are similar to those found in the literature for other selenite phases.[12,13]

Luminescence measurements of the Mn(II) ions in compounds **1** and **2** have been carried out at 6.0 K. The emission spectra for both phases obtained under a 415 nm excitation exhibit a unique red emission at approximately 690 nm. This emission is characteristic of Mn(II) (d^5) octahedrally coordinated (Fig. 3a). The excitation spectra obtained with λ_{em}. of 680 nm reveal the spectral distribution of bands corresponding to

Table 2 Selected bond angles (°) for **1** (e.s.d.s in parentheses)

$Mn(1)O_6$ octahedron		$Mn(2)O_6$ octahedron	
O(5)–Mn(1)–O(1)	102.4(6)	O(1)–Mn(2)–O(6)^{iii}	96.3(6)
O(5)–Mn(1)–O(3)	96.0(6)	O(6)^{iii}–Mn(2)–O(13)	92.1(6)
O(5)–Mn(1)–O(6)^{i}	76.1(5)	O(1)–Mn(2)–O(2)	79.1(6)
O(1)–Mn(1)–O(6)^{i}	99.1(5)	O(13)–Mn(2)–O(2)	91.2(6)
O(3)–Mn(1)–O(6)^{i}	108.1(5)	O(1)–Mn(2)–O(7)^{ii}	86.7(6)
O(5)–Mn(1)–O(4)	101.6(6)	O(6)^{iii}–Mn(2)–O(7)^{ii}	108.4(6)
O(1)–Mn(1)–O(4)	84.8(5)	O(13)–Mn(2)–O(7)^{ii}	95.8(6)
O(3)–Mn(1)–O(4)	68.4(5)	O(2)–Mn(2)–O(7)^{ii}	89.7(6)
O(1)–Mn(1)–O(2)	77.0(6)	O(1)–Mn(2)–O(5)^{i}	89.0(6)
O(3)–Mn(1)–O(2)	93.5(6)	O(6)^{iii}–Mn(2)–O(5)^{i}	76.2(5)
O(6)^{i}-Mn(1)–O(2)	84.3(5)	O(13)–Mn(2)–O(5)^{i}	87.7(6)
O(4)–Mn(1)–O(2)	98.2(5)	O(2)–Mn(2)–O(5)^{i}	84.5(5)
O(1)–Mn(1)–O(3)	150.1(5)	O(1)–Mn(2)–O(13)	170.0(7)
O(6)^{i}-Mn(1)–O(4)	178.5(6)	O(6)^{iii}–Mn(2)–O(2)	161.1(6)
O(5)–Mn(1)–O(2)	160.1(5)	O(7)^{ii}–Mn(2)–O(5)^{i}	174.1(6)
$Mn(3)O_6$ octahedron		$Mn(4)O_6$ octahedron	
O(9)^{iv}–Mn(3)–O(14)	95.2(6)	O(11)^{ii}–Mn(4)–O(15)	96.2(6)
O(9)^{iv}–Mn(3)–O(10)	102.9(6)	O(11)^{ii}–Mn(4)–O(10)	97.9(5)
O(9)^{iv}–Mn(3)–O(7)	100.2(6)	O(11)^{ii}–Mn(4)–O(4)^{ii}	102.7(6)
O(14)–Mn(3)–O(7)	89.2(6)	O(15)–Mn(4)–O(4)^{ii}	95.2(6)
O(10)–Mn(3)–O(7)	87.6(6)	O(10)–Mn(4)–O(4)^{ii}	89.8(5)
O(14)–Mn(3)–O(8)	88.8(5)	O(15)–Mn(4)–O(8)	88.3(6)
O(10)–Mn(3)–O(8)	74.2(6)	O(10)–Mn(4)–O(8)	76.0(6)
O(7)–Mn(3)–O(8)	99.1(5)	O(4)^{ii}–Mn(4)–O(8)	91.4(5)
O(9)^{iv}–Mn(3)–O(11)^{v}	75.7(5)	O(11)^{ii}–Mn(4)–O(9)^{v}	76.2(5)
O(14)–Mn(3)–O(11)^{v}	84.9(5)	O(15)–Mn(4)–O(9)^{v}	83.5(6)
O(10)–Mn(3)–O(11)^{v}	99.5(5)	O(10)–Mn(4)–O(9)^{v}	91.8(6)
O(8)–Mn(3)–O(11)^{v}	85.4(5)	O(8)–Mn(4)–O(9)^{v}	89.9(5)
O(14)–Mn(3)–O(10)	161.9(6)	O(15)–Mn(4)–O(10)	163.6(6)
O(9)^{iv}–Mn(3)–O(8)	160.3(6)	O(11)^{ii}–Mn(4)–O(8)	164.7(5)
O(7)–Mn(3)–O(11)^{v}	172.5(6)	O(4)^{ii}–Mn(4)–O(9)^{v}	178.1(7)
$Se(1)O_3$ trigonal pyramid		$Se(2)O_3$ trigonal pyramid	
O(11)–Se(1)–O(1)	103.0(8)	O(8)–Se(2)–O(2)	103.8(6)
O(11)–Se(1)–O(9)	100.9(8)	O(8)–Se(2)–O(12)	98.2(8)
O(1)–Se(1)–O(9)	99.9(8)	O(2)–Se(2)–O(12)	99.8(7)
$Se(3)O_3$ trigonal pyramid		$Se(4)O_3$ trigonal pyramid	
O(6)–Se(3)–O(10)^{iv}	102.4(8)	O(4)–Se(3)–O(7)	101.4(8)
O(6)–Se(3)–O(5)	101.7(8)	O(4)–Se(3)–O(3)	92.9(7)
O(10)^{iv}–Se(3)–O(5)	100.9(7)	O(7)–Se(3)–O(3)	100.9(7)

Symmetry codes: i = $-x + 1$, $y - 1/2$, $-z + 2$; ii = $-x$, $y - 1/2$, $-z + 2$; iii = x, $y - 1$, z; iv = $-x$, $y + 1/2$, $-z + 2$; v = x, y, $z + 1$; vi = $-x + 1$, $y + 1/2$, $-z + 2$.

the excited levels of Mn(II) in octahedral sites[14,15] [$^4T_1(^4G)$: 537 nm; $^4T_2(^4G)$: 445; $^4A_1,^4E(^4G)$: 414; $^4T_2(^4D)$: 366; $^4E(^4D)$: 344 nm for **1** and $^4T_1(^4G)$: 535; $^4T_2(^4G)$: 443; $^4A_1,^4E(^4G)$: 419; $^4T_2(^4D)$: 358; $^4E(^4D)$: 340 nm for **2**] (Fig. 3b).

The diffuse reflectance spectra of **1** and **2** exhibit several very weak spin-forbidden d–d bands, at approximately 345, 365, 410, 440 and 535 nm for **1** and 345, 355, 420, 440 and 520 nm for **2**. The position of these bands is similar to that obtained from the luminescence results and can be assigned to the Mn(II) ions in octahedral geometry.

Taking into account the results of the luminescence and diffuse reflectance spectroscopies, the *Dq* and Racah parameters have been calculated by fitting the experimental frequencies to an energy level diagram for a high spin octahedral d^5 system.[16] The values obtained are $Dq = 715$, $B = 705$ and $C = 3420$ cm^{-1} for **1** and $Dq = 710$, $B = 700$ and $C = 3425$ cm^{-1} for **2**. Similar values have been found in other octahedrally coordinated Mn(II) compounds.[17] For both selenites the *B*-value is approximately 70% of that corresponding to the free Mn(II) cation (960 cm^{-1}), which indicates a significant degree of covalence in the Mn–O bonds.

ESR and magnetic behaviour

The ESR spectra of **1** and **2** were performed at the X-band on a powdered sample both at room temperature and at 4.2 K. The spectra exhibit isotropic signals due to the presence of high spin Mn(II) cations in a slightly distorted octahedral geometry. The *g*-value for both compounds is 2.00(1) remaining unchanged with variation in temperature.

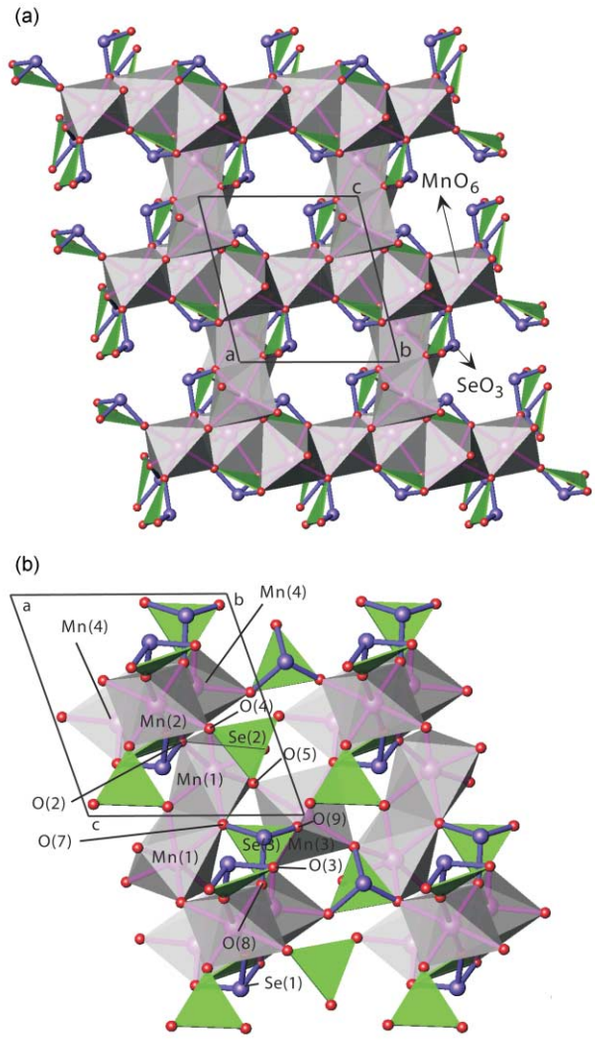

Fig. 2 (a) Polyhedral view of the three-dimensional crystal structure of **2**. (b) Zig-zag chains running along the *a*-axis.

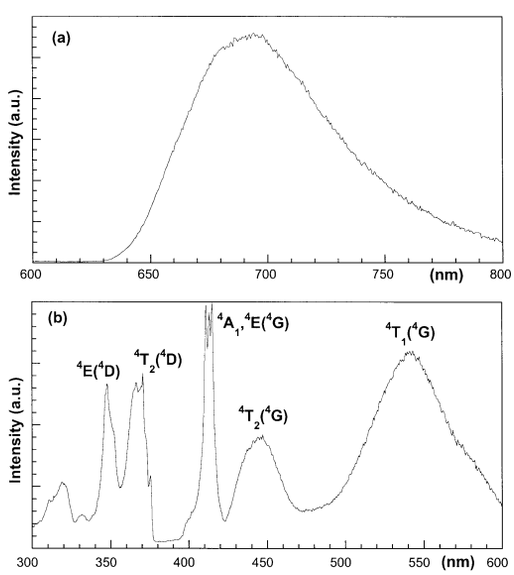

Fig. 3 (a) Luminescent emission spectrum and (b) excitation spectrum of **1** at 6.0 K.

Table 3 Selected bond distances (Å) for **2** (e.s.d.s in parentheses)

$Mn(1)O_6$ octahedron		$Mn(2)O_6$ octahedron	
Mn(1)–O(2)^{i}	2.185(3)	Mn(2)–O(1)	2.205(3)
Mn(1)–O(4)	2.250(4)	Mn(2)–O(1)^{iii}	2.205(3)
Mn(1)–O(5)	2.187(3)	Mn(2)–O(4)	2.186(3)
Mn(1)–O(7)	2.174(4)	Mn(2)–O(4)^{iii}	2.186(3)
Mn(1)–O(7)^{ii}	2.201(4)	Mn(2)–O(8)^{ii}	2.127(4)
Mn(1)–O(10)	2.212(4)	Mn(2)–O(8)^{iv}	2.127(4)
$Mn(3)O_6$ octahedron		$Mn(4)O_6$ octahedron	
Mn(3)–O(3)^{v}	2.256(4)	Mn(4)–O(1)	2.223(4)
Mn(3)–O(3)^{vi}	2.256(4)	Mn(4)–O(2)	2.398(4)
Mn(3)–O(5)	2.141(3)	Mn(4)–O(2)^{i}	2.445(4)
Mn(3)–O(5)^{vii}	2.141(3)	Mn(4)–O(3)^{i}	2.178(4)
Mn(3)–O(9)	2.125(4)	Mn(4)–O(6)^{viii}	2.061(3)
Mn(3)–O(9)^{vii}	2.125(4)	Mn(4)–O(8)^{ii}	2.116(4)
$Se(1)O_3$ trigonal pyramid		$Se(1)O_3$ trigonal pyramid	
Se(1)–O(1)	1.682(4)	Se(2)–O(4)	1.704(3)
Se(1)–O(2)	1.724(4)	Se(2)–O(5)	1.708(4)
Se(1)–O(3)	1.689(3)	Se(2)–O(6)	1.683(4)
$Se(1)O_3$ trigonal pyramid			
Se(3)–O(7)	1.711(3)		
Se(3)–O(8)	1.705(4)		
Se(3)–O(9)	1.656(4)		
Metal–metal			
Mn(1)–Mn(1)^{ii}	3.490(2)	Mn(2)–Mn(4)^{iii}	3.407(1)
Mn(2)–Mn(1)^{iii}	3.918(2)	Mn(3)–Mn(4)^{ix}	3.663(2)
Mn(3)–Mn(1)^{vii}	3.851(1)	Mn(4)–Mn(4)^{i}	3.615(2)
Mn(1)–Mn(4)^{i}	4.199(1)		

Symmetry codes: i = $-x$, $-y + 1$, $-z + 1$; ii = $-x$, $-y + 1$, $-z + 2$; iii = $-x + 1$, $-y + 1$, $-z + 1$; iv = $x + 1$, y, $z - 1$; v = x, y, $z + 1$; vi = $-x$, $-y + 2$, $-z + 1$; vii = $-x$, $-y + 2$, $-z + 2$; viii = x, $y - 1$, z; ix = x, $y + 1$, z.

Table 4 Selected bond angles (°) for **2** (e.s.d.s in parentheses)

$Mn(1)O_6$ octahedron		$Mn(2)O_6$ octahedron	
O(7)–Mn(1)–O(2)^{i}	101.1(1)	O(8)^{iv}–Mn(2)–O(4)	93.0(1)
O(7)–Mn(1)–O(5)	92.6(1)	O(8)^{ii}–Mn(2)–O(4)	87.0(1)
O(7)–Mn(1)–O(7)^{ii}	74.2(1)	O(8)^{iv}–Mn(2)–O(4)^{iii}	87.0(1)
O(2)^{i}–Mn(1)–O(7)^{ii}	95.2(1)	O(8)^{ii}–Mn(2)–O(4)^{iii}	93.0(1)
O(5)–Mn(1)–O(7)^{ii}	97.7(1)	O(8)^{iv}–Mn(2)–O(1)	103.7(1)
O(7)–Mn(1)–O(10)	88.8(2)	O(8)^{ii}–Mn(2)–O(1)	76.3(1)
O(2)^{i}–Mn(1)–O(10)	86.2(1)	O(4)–Mn(2)–O(1)	93.0(1)
O(5)–Mn(1)–O(10)	84.6(1)	O(4)^{iii}–Mn(2)–O(1)	86.9(1)
O(2)^{i}–Mn(1)–O(4)	99.6(1)	O(8)^{iv}–Mn(2)–O(1)^{iii}	76.3(1)
O(5)–Mn(1)–O(4)	68.6(1)	O(8)^{ii}–Mn(2)–O(1)^{iii}	103.7(1)
O(7)^{ii}–Mn(1)–O(4)	96.2(1)	O(4)–Mn(2)–O(1)^{iii}	86.9(1)
O(10)–Mn(1)–O(4)	100.3(2)	O(4)^{iii}–Mn(2)–O(1)^{iii}	93.0(1)
O(2)^{i}–Mn(1)–O(5)	163.3(1)	O(8)^{iv}–Mn(2)–O(8)^{ii}	180.0(0)
O(7)^{ii}–Mn(1)–O(10)	162.9(2)	O(4)–Mn(2)–O(4)^{iii}	180.0(0)
O(7)–Mn(1)–O(4)	157.9(1)	O(1)–Mn(2)–O(1)^{iii}	180.0(0)
$Mn(3)O_6$ octahedron		$Mn(4)O_6$ octahedron	
O(9)^{vii}–Mn(3)–O(5)^{vii}	95.8(1)	O(6)^{viii}–Mn(4)–O(8)^{ii}	103.2(1)
O(9)–Mn(3)–O(5)^{vii}	84.2(1)	O(6)^{viii}–Mn(4)–O(3)^{i}	90.7(1)
O(9)^{vii}–Mn(3)–O(5)	84.2(1)	O(8)^{ii}–Mn(4)–O(3)^{i}	114.7(1)
O(9)–Mn(3)–O(5)	95.8(1)	O(6)^{viii}–Mn(4)–O(1)	110.7(1)
O(9)^{vii}–Mn(3)–O(3)^{v}	87.2(1)	O(8)^{ii}–Mn(4)–O(1)	76.1(1)
O(9)–Mn(3)–O(3)^{v}	92.8(1)	O(6)^{viii}–Mn(4)–O(2)	93.9(1)
O(5)^{vii}–Mn(3)–O(3)^{v}	89.6(1)	O(3)^{i}–Mn(4)–O(2)	98.7(1)
O(5)–Mn(3)–O(3)^{v}	90.4(1)	O(1)–Mn(4)–O(2)	65.9(1)
O(9)^{vii}–Mn(3)–O(3)^{vi}	92.8(1)	O(8)^{ii}–Mn(4)–O(2)^{i}	93.1(1)
O(9)–Mn(3)–O(3)^{vi}	87.2(1)	O(3)^{i}–Mn(4)–O(2)^{i}	66.3(1)
O(5)^{vii}–Mn(3)–O(3)^{vi}	90.4(1)	O(1)–Mn(4)–O(2)^{i}	90.0(1)
O(5)–Mn(3)–O(3)^{vi}	89.6(1)	O(2)–Mn(4)–O(2)^{i}	83.5(1)
O(9)^{vii}–Mn(3)–O(9)	180.0(0)	O(3)^{i}–Mn(4)–O(1)	153.7(1)
O(5)^{vii}–Mn(3)–O(5)	180.0(0)	O(8)^{ii}–Mn(4)–O(2)	141.8(1)
O(3)^{v}–Mn(3)–O(3)^{vi}	180.0(0)	O(6)^{viii}–Mn(4)–O(2)^{i}	156.0(1)
$Se(1)O_3$ trigonal pyramid		$Se(2)O_3$ trigonal pyramid	
O(1)–Se(1)–O(3)	103.6(1)	O(6)–Se(2)–O(4)	101.3(2)
O(1)–Se(1)–O(2)	95.3(2)	O(6)–Se(2)–O(5)	104.5(2)
O(3)–Se(1)–O(2)	96.1(2)	O(4)–Se(2)–O(5)	94.2(2)
$Se(3)O_3$ trigonal pyramid			
O(9)–Se(3)–O(8)	99.8(2)		
O(9)–Se(3)–O(7)	104.8(2)		
O(8)–Se(3)–O(7)	99.5(2)		

Symmetry codes: i = $-x$, $-y + 1$, $-z + 1$; ii = $-x$, $-y + 1$, $-z + 2$; iii = $-x + 1$, $-y + 1$, $-z + 1$; iv = $x + 1$, y, $z - 1$; v = x, y, $z + 1$; vi = $-x$, $-y + 2$, $-z + 1$; vii = $-x$, $-y + 2$, $-z + 2$; viii = x, $y - 1$, z; ix = x, $y + 1$, z.

Magnetic measurements of compounds **1** and **2** were performed on a powdered sample from room temperature to 5.0 K. The thermal evolution of the χ_m and $\chi_m T$ curves is presented in Fig. 4. The molar magnetic susceptibility, χ_m, increases with decreasing temperature and reaches a maximum at 18.4 and 14.0 K, for **1** and **2**, respectively. Below these temperatures the susceptibility continuously decreases with cooling. The thermal variation of the molar susceptibility follows the Curie–Weiss law [$\chi_m = C_m/(T - \theta)$] above *ca.* 30 K for both compounds. The values of the Curie and Curie–Weiss constants are 17.6 cm^3 K mol^{-1} and −31.6 K for **1**, and 13.4 cm^3 K mol^{-1} and −57.7 K for **2**. The $\chi_m T$ *vs.* T curves continuously decrease from room temperature indicating, together with the negative Weiss-temperature, the existence of antiferromagnetic interactions in these compounds.

For **1** the molar magnetic susceptibility in the maximum of the χ_m *vs.* T curve is 2/3 of the magnetic susceptibility extrapolated at 0 K. This result and the structural features suggest the presence of a three-dimensional magnetic system.[18] In this way, the magnetic data of **1** were fitted to a model for a Heisenberg antiferromagnetic three-dimensional simple cubic network of spin $S = 5/2$, by using the Rushbrooke and Wood equation,[19] [eqn. (1)],

$$\chi_m = (35N\beta^2g^2/12kT)(1 + 35x + 221.67x^2 + 608.22x^3 + 26049.6x^4 + 210986.5x^5 + 80149806x^6)^{-1} \quad (1)$$

where $x = |J|/kT$, k is the Boltzmann constant, N is Avogadro's number and β is the Bohr magneton. The best fit of the experimental data to the above equation, represented by the solid line in Fig. 4a, was obtained for $J/k = -0.85$ K considering $g = 2.00$ from the ESR data. These results indicate that compound **1** is well described as a three-dimensional antiferromagnet.

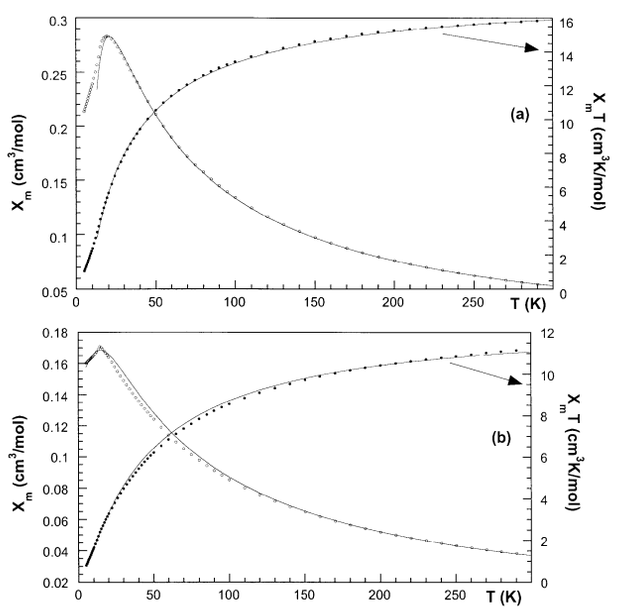

Fig. 4 Thermal variation of the χ_m and $\chi_m T$ curves for (a) **1** and (b) **2**.

Table 5 Selected bands (in cm^{-1}) from the IR and Raman spectra of **1** and **2**

	1		**2**	
Assignment	IR	Raman	IR	Raman
$\nu(H_2O)$	3370–2920 (m)	—	3525–2920 (m)	—
$\delta(H_2O)$	1630 (w)	—	1615 (w)	—
$\nu_s(SeO_3)^{2-}$	950 (m)	835 (s)	865, 830 (m)	865, 835, 820 (s)
$\nu_{as}(SeO_3)^{2-}$	730, 705 (s)	805, 750 (m,w)	760, 705 (s)	765, 710, 700 (d)
$\delta(SeO_3)^{2-}$	455 (m)	460, 420, 385, 315 (w)	515, 485, 430 (m)	515, 485, 430 (w)

ν = stretching; δ = deformation; s = symmetric; as = asymmetric; w = weak; m = medium; s = strong; sh = shoulder.

Attempts to fit the magnetic data of compound **2** to a simple cubic network were unsuccessful. From the magnetic point of view we can consider a system formed by chains running along the crystallographic *a*-axis, in accordance with the structural results. Therefore, the magnetic data were fitted to the equation given by Fisher and Dingle[20] for chains of spin $S = 5/2$, [eqn. (2)]

$$\chi = [Ng^2\beta^2S(S + 1)/3kT][(1 - n)/(1 + n)] \qquad (2)$$

where $n = (T/T_0) - \coth(T_0/T)$ and $T_0 = [2JS(S + 1)]/k$. The best fit, indicated by the solid line in Fig. 4b, was obtained with $J/k = -1.75$ K, $g = 1.99$ and considering a J'-exchange parameter between neighbour chains of -0.75 K. The high value obtained for the J'-parameter suggests that the fit must be considered with caution. In this way, the main magnetic interactions could be propagated along the chains. However, other magnetic contributions, probably three-dimensional in nature, must take into account the low temperature region to explain the magnetic behaviour of **2** in a satisfactory way.

Several magnetic exchange pathways can take place in compounds **1** and **2** (see Figs. 1 and 2): (i) intradimeric direct interactions in the Mn_2O_{10} edge-sharing dimeric octahedra along the chains involving the d_{xz} orbitals of the Mn^{2+} cations. (ii) superexchange intradimer interactions *via* oxygen involving metal $d_{x^2-y^2}$ orbitals from edge-sharing dimeric octahedra. (iii) superexchange interactions *via* vertex oxygen atoms between the Mn(II) ions in the three-dimensional framework. (iv) superexchange interactions through the $(SeO_3)^{2-}$ anions which are linked to the MnO_6 polyhedra in three dimensions. The values of the dihedral and bond angles involved in these exchange pathways are near to 180 and 110°, respectively, for exchange pathways (i), (ii) and (iii). These values should lead to predominant antiferromagnetic interactions in these compounds.[21] Finally, the superexchange pathways through the oxoanions should also favour the antiferromagnetic couplings, as observed in other related compounds.[22]

Concluding remarks

Two new manganese(II) selenites with formulae $Mn_4(H_2O)_3(SeO_3)_4$ and $Mn_3(H_2O)(SeO_3)_3$ have been synthesized by using mild hydrothermal techniques. The compounds show three-dimensional networks constructed from MnO_6 octahedra and $(SeO_3)^{2-}$ anions with trigonal pyramidal geometry. Layers formed by zig-zag chains can be distinguished in the structures. The IR spectra show the presence of water molecules and selenite anions. The diffuse reflectance and luminescence spectra indicate the existence of manganese(II) ions in a slightly distorted octahedral symmetry. The ESR spectra are isotropic, in good agreement with the geometry of the metallic cations in these compounds. Magnetic measurements indicate the existence of antiferromagnetic interactions. The magnetic behaviour of $Mn_4(H_2O)_3(SeO_3)_4$ has been interpreted on the basis of an isotropic simple cubic three-dimensional framework. In the case of $Mn_3(H_2O)(SeO_3)_3$, the magnetic data have been fitted considering that the main magnetic interactions are propagated along the manganese(II) chains.

Experimental

Synthesis and characterization

Compounds **1** and **2** have been synthesized using mild hydrothermal conditions under autogeneous pressure. Compound **1** was prepared from SeO_2 (1.26 mmol) and $MnCl_2{\cdot}4H_2O$ (0.126 mmol) (ratio Se : Mn = 10) in 30 ml of water. The pH of the reaction mixture was increased up to 5.5 by using ethylenediamine and the mixture was stirred until homogeneous. After that, the reagents were sealed in a PTFE-lined stainless steel pressure vessel (fill factor 75%) and heated at 170 °C for 3 hours, followed by slow cooling to room temperature. The pH was practically constant during the hydrothermal reaction and remained at 5.5. Light-pink single-crystals appeared which were isolated by filtration, washed with water and acetone and dried over P_2O_5 for 2 h. Attempts performed under the same conditions but with longer reaction times led to a mixture of phases. The powder X-ray diffraction pattern indicates the existence of compound **1** and other manganese(II) compounds belonging to the $M_3(H_2O)(SeO_3)_3$ family.[4a]

In order to obtain compound **2** as a pure phase, several experimentals with different Se : Mn ratios, pH and reaction times were carried out. In this way, compound **2** was synthesized from SeO_2 (9.00 mmol) and $Mn(SO_4){\cdot}H_2O$ (1.40 mmol) [ratio Se : Mn = 6.4] in 30 ml of water, the pH being increased up to 5.0 with ammonium hydroxide. These reagents were sealed in a PTFE-lined stainless steel pressure vessel (fill factor 75%) and heated at 170 °C for 72 h. No variation in the pH of the reaction was observed. Light-pink single-crystals appeared which were isolated by filtration, washed with water and acetone and dried over P_2O_5 for 2 h.

The manganese and selenium contents of both phases were confirmed by inductively coupled plasma atomic emission spectroscopy (ICP-AES) analysis. Compound **1**, Found: Mn, 27.1; Se, 38.7. Required Mn, 27.5; Se, 39.5%. Compound **2**, Found: Mn, 29.0; Se, 41.8. Required Mn, 29.2; Se, 42.0%. The obtained value of the density, measured by picnometry, was 3.6(1) g cm^{-3} for both compounds.

Thermogravimetric analysis of these compounds was carried out under air in a SDC 2960 Simultaneous DSC-TGA TA instrument. Crucibles containing *ca.* 20 mg of sample were heated at 5 °C min^{-1} in the temperature range 30–800 °C. The decomposition curves of both phases revealed a continuous weight loss in the 200–350 and 250–400 °C ranges for **1** and **2**, respectively. These steps correspond to the elimination water (calculated: 7.0, 3.2; required: 7.3, 3.5%). The complete decomposition of **1** and **2** takes place in the *ca.* 450–600 °C range. Mn_2O_3 [*Ia*3 space group with $a = 9.43$ Å][23a] was the only product detected in the X-ray powder diffraction patterns of the thermogravimetric residues at 800 °C.

The thermal behaviour of compounds **1** and **2** was also studied by using time-resolved X-ray thermodiffractometry in air. A PHILIPS X'PERT automatic diffractometer (Cu-Kα

Table 6 Crystallographic data and details of crystal structure refinement for **1** and **2**

Compound	**1**	**2**
Chemical formula	$H_6Se_4Mn_4O_{15}$	$H_2Se_3Mn_3O_{10}$
Formula weight/g mol^{-1}	781.65	563.72
Crystal system	Monoclinic	Triclinic
Space group	$P2_1$ (no. 4)	$P\bar{1}$ (no. 2)
a/Å	9.181(2)	8.266(3)
b/Å	8.602(3)	8.350(3)
c/Å	9.852(4)	9.008(3)
α/°	90	65.24(3)
β/°	116.63(2)	68.82(4)
γ/°	90	67.77(4)
V/Å^3	695.5(4)	507.2(3)
Z	2	2
T/°C	20	20
Radiation, λ(Mo-Kα)/Å	0.71070	0.71070
μ(Mo-Kα), mm^{-1}	14.093	14.478
Measured reflections	1334	3221
Independent	1290 [R_{int} = 0.04]	1620 [R_{int} = 0.02]
Observed [$I > 2\sigma(I)$]	1204	1344
R [$I > 2\sigma(I)$]	$R1$ = 0.056, $wR2$ = 0.152	$R1$ = 0.022, $wR2$ = 0.047
R [all data]	$R1$ = 0.060, $wR2$ = 0.156	$R1$ = 0.031, $wR2$ = 0.049

$R1 = [\Sigma(|F_o| - |F_c|)]/\Sigma|F_o|$; $wR2 = [\Sigma[w(|F_o|^2 - |F_c|^2)^2]/\Sigma[w(|F_o|^2)^2]^{1/2}$; $w = 1/[\sigma^2|F_o|^2 + (xp)^2 + yp]$; where $p = [|F_o|^2 + 2|F_c|^2]/3$; $x = 0.0857$, $y = 11.96$ for compound **1** and $x = 0.0277$ for compound **2**.

radiation) equipped with a variable-temperature stage (Paar Physica TCU2000) with a Pt sample holder was used. The powder patterns were recorded in 2θ steps of 0.02° in the range $5 \leq 2\theta \leq 40°$, counting for 2 s per step and increasing the temperature at 5 °C min^{-1} from room temperature up to 700 °C. Compound **1** is stable up to *ca.* 195 °C. A strong decrease of the peak intensities takes place in the 195–345 °C range, indicating the beginning of decomposition in the compound. Between 345 and 380 °C, peaks belonging to the metallic selenium [$P2_1/a$ space group with a = 12.85, b = 8.07, c = 9.31 Å and β = 93.13°][23b] and the Mn(SeO_3) phase [*Pnma* space group with a = 6.0945(4), b = 7.8656(8), c = 5.1460(4) Å][23c] were observed in the X-ray diffraction patterns. At temperatures higher than *ca.* 400 °C the Mn_2O_3 oxide[23a] was detected. Compound **2** is stable up to *ca.* 255 °C. The $MnMn_2O(SeO_3)_3$ phase [*C*2/*m* space group with a = 15.4540(4), b = 6.6520(2), c = 9.6820(2) Å and β = 118.83(1)°][23d] appears in the 255–390 °C range. Above 400 °C, the Mn_2O_3 oxide[23a] is formed. These results are in good agreement with those obtained from the thermogravimetric study.

X-Ray diffraction study

Prismatic single-crystals of **1** and **2** with dimensions 0.4 × 0.07 × 0.02 and 0.08 × 0.05 × 0.06 mm., respectively, and relatively good quality were carefully selected under a polarizing microscope and mounted on a glass fiber. Diffraction data of **1** and **2** were collected at room temperature on an Enraf-Nonius CAD4 and a STOE IPDS (Imaging Plate Diffraction System) automated diffractometers, respectively, using graphite-monochromatic Mo-Kα radiation. Details of crystal data, intensity collection and some features of the structure refinement are reported in Table 6. Corrections for Lorentz and polarization effects of **1** were done and also for absorption with the empirical ψ scan method[24] by using the XRAYACS program.[25] The software of the STOE IPDS diffractometer[26] was used to perform the corrections for Lorentz and polarization effects of **2**. The absorption corrections in compound **2** were carried out by using the XRED program.[27] The structures were solved by the Patterson method (SHELXS 86 program)[28] and refined by full-matrix least-squares based on F^2, using the SHELXL 97 computer program.[29] The scattering factors were taken from ref. 30. Anisotropic thermal parameters were assigned to the non-hydrogen atoms, except for the oxygen atoms of **1** which were isotropically refined. The hydrogen atoms belonging to the water molecules of **1** were not found. In the case of **2** they were located in the difference Fourier maps. All drawings were made using the ATOMS program.[31]

CCDC reference numbers 181273 and 181274.

See http://www.rsc.org/suppdata/dt/b2/b206515k/ for crystallographic data in CIF or other electronic format.

Physicochemical characterization techniques

The IR spectra (KBr pellets) were obtained with a Nicolet FT-IR 740 spectrophotometer in the 400–4000 cm^{-1} range. The Raman spectra were recorded in the 200–3000 cm^{-1} range, with a Nicolet 950FT spectrophotometer equipped with a neodymium laser emitting at 1064 nm. Luminescence measurements were carried out in a Spectrofluorimeter Fluorolog-2 SPEX 1680, model F212I at 6.0 K. The excitation source was a high pressure xenon lamp emitting between 200 and 1200 nm. Diffuse reflectance spectra were registered at room temperature on a Cary 2415 spectrometer in the 210–2000 nm range. A Bruker ESP 300 spectrometer was used to record the ESR polycrystalline spectra. The temperature was stabilized with an Oxford Instrument (ITC 4) regulator. The magnetic field was measured with a Bruker BNM 200 gaussmeter and the frequency inside the cavity was determined using a Hewlett-Packard 5352B microwave frequency counter. Magnetic measurements on powdered samples were performed in the temperature range 5.0–300 K, using a Quantum Design MPMS-7 SQUID magnetometer. The magnetic field was approximately 0.1 T, a value in the range of linear dependence of magnetization *vs.* magnetic field even at 5.0 K.

Acknowledgements

This work was financially supported by the Ministerio de Educación y Ciencia (PB97-0640; BQU2001-0678) and Universidad del País Vasco/EHU (9/UPV00169.310-13494/2001; 9/UPV00130.310-13700/2001), which we gratefully acknowledge. One of us, A. Larrañaga, wishes to thank the Gobierno Vasco/Eusko Jaurlaritza for funding.

References

1 S. M. Kauzlarich, P. K. Dorhout and J. M. Honig, *J. Solid State Chem.*, 2000, **149**, 3.

2 M. Koskenlinna, *Structural Features of Selenium*(IV) Oxoanions Compounds, J. Koskikallio, ed., Helsinki University of Technology, 1996.
3 (*a*) B. Engelen, K. Boldt, K. Unterderweide and U. Baumer, *Z. Anorg. Allg. Chem.*, 1995, **621**, 331; (*b*) M. Koskenlinna, J. Kansikas and T. Leskela, *Acta Chem. Scand.*, 1994, **48**, 783; (*c*) Z. Micka, I. Nemec, P. Vojtisek, J. Ondracek and J. Holsa, *J. Solid State Chem.*, 1994, **112**, 237; (*d*) J. Valkonen and M. Koskenlinna, *Acta Chem. Scand., Ser. A*, 1978, **32**, 603; (*e*) W. T. A. Harrison, G. D. Stucky and A. K. Cheetham, *Eur. J. Solid State Inorg. Chem.*, 1993, **30**, 347.
4 (*a*) M. Wildner, *Monatsh. Chem.*, 1991, **122**, 585; (*b*) A. V. P. McManus, W. T. A. Harrison and A. K. Cheetham, *J. Solid State Chem.*, 1991, **92**, 253; (*c*) H. Effenberger, *J. Solid State Chem.*, 1987, **70**, 303; (*d*) W. T. A. Harrison, G. D. Stucky, R. E. Morris and A. K. Cheetham, *Acta Crystallogr., Sect. C*, 1992, **48**, 1365.
5 (*a*) M. Koskenlinna, L. Niinisto and J. Valkonen, *Acta Chem. Scand., Ser. A*, 1976, **30**, 836; (*b*) G. Meunier and M. Bertaud, *Acta Crystallogr., Sect. B*, 1974, **30**, 2840; (*c*) F. C. Hawthorne, L. A. Groat and T. S. Ercit, *Acta Crystallogr., Sect. C*, 1987, **43**, 2042; (*d*) W. T. A. Harrison, A. V. P. McManus and A. K. Cheetham, *Acta Crystallogr., Sect. C*, 1992, **48**, 412.
6 (*a*) H. Muilu and J. Valkonen, *Acta Chem. Scand., Ser. A*, 1987, **41**, 183; (*b*) Z. Micka, I. Nemec, P. Vojtisek, J. Ondracek and J. Holsa, *J. Solid State. Chem.*, 1994, **112**, 237; (*c*) J. Bonvoisin, J. Galy and J.C. Trombe, *J. Solid State Chem.*, 1993, **170**, 171.
7 (*a*) J. L. Pizarro, M. I. Arriortua, L. Lezama, T. Rojo and G. Villeneuve, *Solid State Ionics*, 1993, **63–65**, 71; (*b*) J. M. Rojo, J. L. Mesa, L. Lezama, J. Rodriguez-Fernandez, J. L. Pizarro, M. I. Arriortua and T. Rojo, *Int. J. Inorg. Mater.*, 2001, **3**, 67; (*c*) J. M. Rojo, J. L. Mesa, J. L. Pizarro, J. Garcia-Tojal, M. I. Arriortua and T. Rojo, *High Press. Res.*, 2002, **22**, 569; (*d*) J. M. Rojo, A. Larrañaga, J. L. Mesa, M. K. Urtiaga, J. L. Pizarro, M. I. Arriortua and T. Rojo, *J. Solid State Chem.*, 2002, **165**, 171.
8 A. K. Cheetham, G. Ferey and T. Loiseau, *Angew. Chem., Int. Ed.*, 1999, **38**, 3268.
9 (*a*) W. T. A. Harrison, M. K. L. Phillips, J. Stanchfield and T. N. Nenoff, *Angew. Chem., Int. Ed.*, 2000, **39**, 3808; (*b*) A. Choudhury, U. Kumar and C. N. R. Rao, *Angew. Chem., Int. Ed.*, 2002, **41**, 158.
10 E. L. Muetterties and L. J. Guggenberger, *J. Am. Chem. Soc.*, 1974, **96**, 1748.
11 I. D. Brown, *Structure and Bonding in Crystals*, M. O'Keeffe and A. Navrotsky, eds., vol. 2, p. 1, Academic Press, New York, 1981.
12 M. Elbert, Z. Micka and I. Pekova, *Collect. Czech. Chem. Commun.*, 1982, **C47**, 2069.
13 K. Nakamoto, *Infrared and Raman Spectra of Inorganic and Coordination Compounds*, John Wiley & Sons: New York, 1997.
14 Y. Tanabe and S. Sugano, *J. Phys. Soc. Jpn.*, 1954, **9**, 753.
15 L. E. Orgel, *J. Chem. Phys.*, 1955, **23**, 1004.
16 A. B. P. Lever, *Inorganic Electronic Spectroscopy*, Elsevier Science Publishers B.V., Amsterdam, Netherlands, 1984.
17 (*a*) K. E. Lawson, *J. Chem. Phys.*, 1966, **44**, 4159; (*b*) J. Escobal, J. L. Mesa, J. L. Pizarro, L. Lezama, R. Olazcuaga and T. Rojo, *J. Mater. Chem.*, 1999, **9**, 2691; (*c*) J. Escobal, J. L. Pizarro, J. L. Mesa, L. Lezama, R. Olazcuaga, M. I. Arriortua and T. Rojo, *Chem. Mater.*, 2000, **12**, 376; (*d*) S. Fernandez, J. L. Mesa, J. L. Pizarro, L. Lezama, M. I. Arriortua, R. Olazcuaga and T. Rojo, *Chem. Mater.*, 2000, **12**, 2092; (*e*) S. Fernandez, J. L. Pizarro, J. L. Mesa, L. Lezama, M. I. Arriortua, R. Olazcuaga and T. Rojo, *Inorg. Chem.*, 2001, **40**, 3476.
18 R. L. Carlin, *Magnetochemistry*, Springer-Verlag, Berlin, Heidelberg, 1986.
19 G. S. Rushbrooke and P. J. Wood, *Mol. Phys.*, 1958, **1**, 257.
20 (*a*) M. E. Fisher, *Am. J. Phys.*, 1964, **32**, 343; (*b*) R. Dingle, M. E. Lines and S. L. Holt, *Phys. Rev.*, 1969, **187**, 643.
21 J. B. Goodenough, *Magnetism and the Chemical Bond*, Interscience, New York, 1963.
22 L. Lezama, K. S. Shu, G. Villeneuve and T. Rojo, *Solid State Commun.*, 1990, **76**, 449.
23 Powder Diffraction File—Inorganic and Organic, ICDD, file nos. (*a*) 78–390, (*b*) 24–714, (*c*) 70–241 and (*d*) 82–1420, Pennsylvania, USA, 1995.
24 A. C. T. North, D. C. Philips and F. S. Mathews, *Acta Crystallogr., Sect. A*, 1968, **24**, 351.
25 A. Chandrasekaran, XRAYACS: Program for Single Crystal X-ray Data Corrections, Chemistry Department, University of Massachusetts, Amherst, USA, 1998.
26 Stoe IPDS Software, version 2.87, Stoe & Cie, Darmstadt, Germany, 1998.
27 XRED, Stoe & Cie GmbH, Darmstadt, Germany, 1998.
28 G. M. Sheldrick, *Acta Crystallogr., Sect. A*, 1990, **46**, 467.
29 G. M. Sheldrick, SHELXL 97: Program for the Refinement of Crystal Structures, University of Göttingen, Germany, 1997.
30 *International Tables for X-Ray Crystallography*, Kynoch Press, Birmingham, England, vol. IV, p. 99, 1974.
31 E. Dowty, ATOMS: A Computer Program for Displaying Atomic Structures, Shape Software, 521 Hidden Valley Road, Kingsport, TN, 1993.